Preliminary NoMAD Results of the MUSIC Experiment

Alexander McSpaden*, Caiser Bravo*†, Theresa Cutler*, Joetta Goda*, Wim Haeck*, Jesson Hutchinson*, Hadyn Kistle*‡, George McKenzie*, William Myers*, Rene Sanchez*, Robert Weldon*

*Los Alamos National Laboratory, P.O. Box 1663, Los Alamos, NM, 87544, mcspaden@lanl.gov
†Nuclear Engineering and Radiological Sciences, University of Michigan, 2355 Bonisteel Blvd, Ann Arbor, MI, 48109
‡Department of Nuclear Engineering, Texas A&M University, 423 Spence St., College Station, TX, 77843

INTRODUCTION

The Measurement of Uranium Subcritical and Critical (MUSiC) experiment was carried out from December 2020 through April 2021 at the National Criticality Experiments Research Center (NCERC). This measurement campaign featured bare configurations of the Rocky Flats highly-enriched uranium (HEU) shells, with each configuration having different numbers of these shells. The goal of the experiment was to test multiple neutron multiplicity detectors and measurement methods for a large range of neutron multiplication values, to see when the combination of detectors and methods break down as the configurations reach the delayed supercritical window [1, 2].

Adding subcritical integral benchmarks gives additional validation to nuclear data. These benchmarks provide additional parameters against which to validate the data. While critical benchmarks have just a single value, k_{eff}, subcritical benchmarks can be used to infer multiple parameters. As an example, recent subcritical benchmarks utilizing the Hage-Cifarelli formalism have three quantities of interest (R_1, R_2, and M_L). This gives nuclear data evaluators additional data to use when performing their evaluations, and allows for these benchmarks to be useful for additional types of nuclear data.

CONFIGURATIONS

The Rocky Flats shells are a set of nesting HEU hemishells that can be used in any number of different ways depending on the experiment [3]. These shells have already been used in International Criticality Safety Benchmark Evaluation Project (ICSBEP) benchmarks, including at Los Alamos [4]. Table I lists the reported initial composition of the Rocky Flats shells. Figure 1 also shows a picture of a subset of these shells. These shells were placed into two separate stacks on the Planet vertical lift machine, where final assembly was done remotely [5]. Figure 2 depicts a configuration of this experiment on Planet. All configurations were measured three times: once with a ^{252}Cf source, once with no external source, and finally with a D-T neutron generator.

Fig. 1. A Subset of the Rocky Flats Shells.

TABLE I. Rocky Flats Shells Reported Composition

Uranium Isotope	Weight Percent
234	1.02
235	93.16
236	0.47
238	5.35

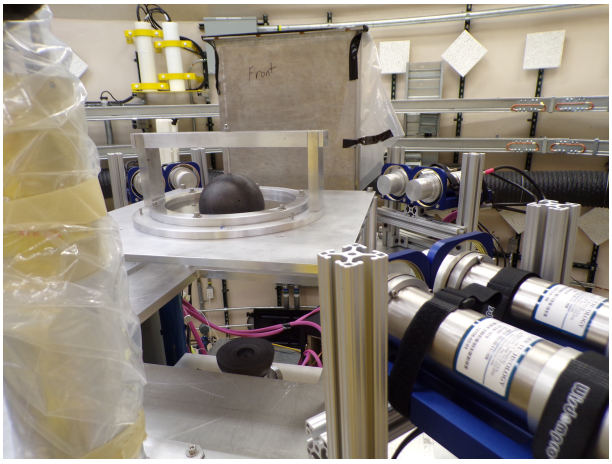

Fig. 2. A Subcritical Configuration Fully Separated on Planet.

Eight total subcritical configurations of the Rocky Flats shells were measured as part of this campaign, along with two critical configurations. The difference between the subcritical configurations were the number of shells that were used and consequently, the neutron multiplication. Table II summarizes the configurations. The space inside the innermost Rocky Flat shell is filled with aluminum, and the very center included a source holder for the ^{252}Cf.

DETECTOR SYSTEMS

Seven separate detector systems were in place for the experiment. The focus of this summary is the Neutron Multiplicity Array Detector (NoMAD) used in the experiment. The placement of this detector and the other detector systems around Planet for the campaign is shown in Figure 3. Two of these systems, the so-called "linears" and "log-N's" are current mode boron-lined compensated ion-chambers that monitor the neutron population. While the log-N's are purely for shutting down the machine if the population reaches a certain level, the linears are used to ascertain the reactor period in a supercritical

TABLE II. MUSiC Subcritical Configurations

Configuration	Rocky Flats Shells	Mass (kg)
1	3-24	13.0428
2	3-30	21.6432
3	3-34	29.0415
4	3-38	37.9617
5	3-40	42.9722
6	3-42	48.4099
7	3-44	54.2785
10	9-46	59.2075

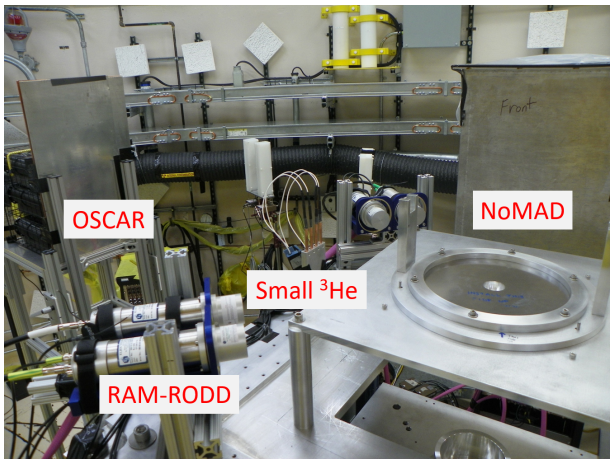

Fig. 3. The Placement of the Detector Systems Around Planet.

system, and find delayed critical if desired as part of the experiment. While these detectors were useful for the approach to critical and for the supercritical configurations, no data from either of these systems will be analyzed for subcritical configurations.

Three of the other detector systems rely on ^{3}He. The "startups" are a set of four tubes that monitor the neutron population at low power levels, used for the approach to critical and measuring the reactor period at very low power levels. A second ^{3}He based detection system is the NoMAD, one of the main multiplicity detectors for the experiment. This system consists of 15 tubes embedded within a high-density polyethylene (HDPE) matrix. This is the same detector system that has been used for previous NCERC subcritical neutron multiplication benchmarks [6, 7, 8]. The output of this detector is a list-mode data file, meaning it has a list of detection events along with their associated times. Figure 4 shows a picture of one of these systems. There was approximately 41.1 cm between the center of the assembly and the front face of the container for the NoMAD.

A third ^{3}He based detection system is a series of four much smaller tubes. Since these tubes are smaller, they have a much decreased efficiency, meaning that at higher powers

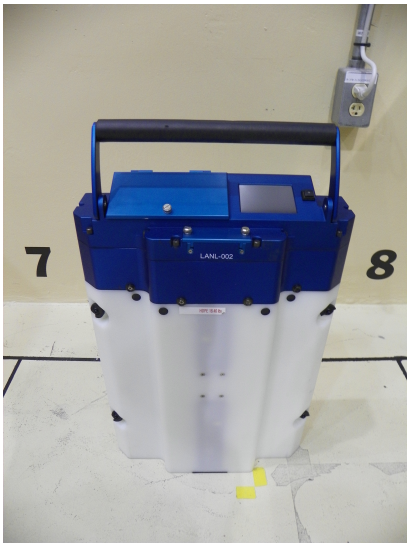

Fig. 4. The NoMAD system.

when the NoMAD or other systems are saturated data collection is still possible. These tubes are primarily used for measuring the Rossi-α of a system near delayed critical. The tubes were placed 40.6 cm away from the center of the assembly

Two organic scintillator arrays were also used for the experiment. One, the OSCAR system, was operated by students from the University of Michigan and consists of a set of trans-stilbene scintillators [9]. The OSCAR was behind the small ^{3}He tubes, 137.5 cm away from the center of the assembly The second set of scintillators is a set of eight EJ-309 liquid scintillators known as RAM-RODD [10]. These detectors were placed in banks of two at the four corners of the top plate of Planet, with the front faces of the scintillators approximately 46.7 cm away from the center of the assembly. The data from these are presented in other summaries submitted to this conference [11, 12].

METHOD

One data analysis technique that can be used on the subcritical data is the Hage-Cifarelli [13] formalism of the Feynman Variance-to-Mean method [14]. This method first creates a Feynman histogram, which involves creating time gates in the measurement and seeing how many neutrons are detected in those gates. The histogram is then made by counting how many times a certain number of neutrons are counted within the bins. The moments of these histograms are then computed for a number of different gate lengths (τ) as shown in Eqs. 1-2 [15].

$$m_1(\tau) = \frac{\Sigma_n n C_n}{\Sigma_n C_n} \tag{1}$$

$$m_2(\tau) = \frac{\Sigma_n n(n-1) C_n}{2\Sigma_n C_n} \tag{2}$$

In the previous equations, n is the number of neutrons in a gate, and C_n is the number of instances of n neutrons being in a gate. Once these moments are computed, they are then used

to infer the count rates R_1 and R_2, which are also known as the "singles" and "doubles" rate. The equations for determining these are given in Eqs. 3-5. In these equations, λ is the inverse neutron lifetime.

$$R_1(\tau) = \frac{m_1(\tau)}{\tau} \tag{3}$$

$$R_2(\tau) = \frac{1}{\tau\omega_2(\tau)}(m_2(\tau) - \frac{1}{2}m_1^2(\tau)) \tag{4}$$

$$\omega_2(\tau) = 1 - \frac{1}{\lambda\tau}(1 - e^{-\lambda\tau}) \tag{5}$$

These count rates are also defined as the rate at which one (R_1) or two (R_2) neutrons are detected from the same fission chain, and the equations governing that definition are given in Eqs. 6-9. Here, F_S is the spontaneous fission rate, ε is the absolute detector efficiency, $\overline{\nu_{Sn}}$ and $\overline{\nu_{In}}$ are the nth reduced factorial moments of the spontaneous and induced fission multiplicity distribution, respectively. The leakage multiplication of the system, defined as the average number of neutrons that leak out of the system for every starter neutron, is in these equations as M_L. It is because of these equations that the leakage multiplication can be inferred from the measured data.

$$R_1 = \varepsilon b_{11} F_s \tag{6}$$

$$b_{11} = M_L\overline{\nu_{S1}} \tag{7}$$

$$R_2 = \varepsilon^2 b_{21} F_S \tag{8}$$

$$b_{21} = M_L^2[\overline{\nu_{S2}} + \frac{M_L - 1}{\overline{\nu_{I1}} - 1}\overline{\nu_{S1}\nu_{I2}}] \tag{9}$$

The data from the list mode detector systems can also be analysed with the Rossi-α and other analysis methods, but that is outside the scope of this summary.

PRELIMINARY RESULTS

The results from the NoMAD detector system using the Hage-Cifarelli formalism are shown in Table III. It should be noted that these are preliminary results, and further analysis will be done as part of submission to the ICSBEP handbook.

It can be seen that as the mass of the configuration increases, naturally the intrinsic source strength increases, leading to a higher count rate and better statistics. The addition of the ^{252}Cf source is extremely beneficial to reducing the statistical error in the results, especially for the low mass configurations.

CONCLUSIONS

The limits of the Hage-Cifarelli formalism are tested through low intrinsic source configurations such as those presented in MUSiC, especially when the mass of the nuclear material is relatively low. Adding an external neutron source makes analysis of these systems much easier, significantly reducing the magnitude of the error.

In the future, the data from the NoMAD detector systems used in this experiment will be analyzed with additional multiplicity analysis methods. This will help determine where the detector systems perform most optimally and identify regimes where different analysis methods may perform better than others. Additionally, a full benchmark analysis of both the critical and subcritical data for this experiment will be submitted to the ICSBEP handbook, beginning with the critical configuration.

ACKNOWLEDGEMENTS

This work was supported by the Department of Energy Nuclear Criticality Safety Program, funded and managed by the National Nuclear Security Administration for the Department of Energy.

REFERENCES

1. A. MCSPADEN, T. CUTLER, J. HUTCHINSON, R. BAHRAN, W. MYERS, G. MCKENZIE, J. GODA, and R. SANCHEZ, "IER 488: Measurement of Uranium Subcritical and Critical (MUSiC) CEDT Phase-2 Final Design," (2018).
2. A. MCSPADEN, T. CUTLER, J. HUTCHINSON, W. MYERS, G. MCKENZIE, J. GODA, and R. SANCHEZ, "MUSIC: A CRITICAL AND SUBCRITICAL EXPERIMENT MEASURING HIGHLY ENRICHED URANIUM SHELLS," *International Conference on Nuclear Criticality 2019* (2019).
3. R. ROTHE, "Extraploated Experimental Critical Parameters of Unreflected and Steel-Reflected Massive Enriched Uranium Metal Spherical and Hemispherical Assemblies," *INEEL report INEEL/EXT-97-01401* (1997).
4. D. LOAIZA, R. BREWER, and R. SANCHEZ, "Neptunium-237 Sphere Surrounded by Hemispherical Shells of Highly Enriched Uranium," *International Handbook of Evaluated Criticality Safety Benchmark Experiments*, **NEA/NSC/DOC/(95)03/I**, SPEC–MET–FAST–008 (2009).
5. R. SANCHEZ and ET. AL., "A New Era of Nuclear Criticality Experiments, The First Ten Years of Planet Operations at NCERC," *Nuclear Science and Engineering*, **Submitted** (2021).
6. B. RICHARD and J. HUTCHINSON, "Nickel Reflected Plutonium Metal Sphere Subcritical Measurements," *In: International Handbook of Evaluated Criticality Safety Benchmark Experiments*, **[DVD]/Nuclear Energy Agency. - Paris : OECD Nuclear Energy Agency** (2016), (NEA;7328).
7. B. RICHARD and J. HUTCHINSON, "Tungsten-Reflected Plutonium-Metal-Sphere Subcritical Measurements," *In: International Handbook of Evaluated Criticality Safety Benchmark Experiments*, **[DVD]/Nuclear Energy Agency. - Paris : OECD Nuclear Energy Agency** (2016), (NEA;7328).
8. T. CUTLER, J. ARTHUR, and J. HUTCHINSON, "Copper and Polyethylene-Reflected Plutonium-Metal-Sphere Subcritical Measurements," *In: International Handbook of Evaluated Criticality Safety Benchmark Experiments*,

TABLE III. Preliminary NoMAD Results for Configurations Without an External Source.

Configuration	Measurement Time (min)	R_1	R_2	M_L
1	90	9.3080 ± 3.841E-7	5.291E-3 ± 3.316E-2	0.62 ± 0.30
2	90	9.9385 ± 4.875E-7	1.408E-2 ± 8.177E-2	0.69 ± 0.57
3	60	10.615 ± 8.916E-7	5.122E-2 ± 2.568E-1	0.88 ± 1.14
4	60	11.999 ± 8.203E-6	2.162E-1 ± 1.04595	1.33 ± 2.34
5	60	13.941 ± 1.889E-6	5.766E-1 ± 2.78817	1.83 ± 3.61
6	90	17.672 ± 9.851E-7	2.290 ± 11.249	2.99 ± 6.57
7	60	33.075 ± 1.836E-6	23.532 ± 121.771	6.60 ± 16.30
10	8	36.120 ± 2.85357	28.119 ± 146.521	6.89 ± 17.172

[DVD]/Nuclear Energy Agency. - Paris : OECD Nuclear Energy Agency (2019), (NEA;7328).

9. M. HUA, C. BRAVO, A. MACDONALD, J. HUTCHINSON, G. MCKENZIE, B. KIEDROWSKI, S. CLARKE, and S. POZZI, "Rossi-alpha measurements of fast plutonium metal assemblies using organic scintillators," *Nuclear Instruments and Methods in Physics Research Section A: Accelerators, Spectrometers, Detectors and Associated Equipment*, **959**, 163507 (2020).
10. R. WELDON, T. CUTLER, J. HUTCHINSON, G. MCKENZIE, L. MISUREK, and E. SORENSEN, "Rossi Alpha Measurements - Rapid Organic (n,γ) Discrimination Detector (RAM-RODD) System Capabilities," (2020).
11. R. WELDON and ET. AL., "Preliminary RAM-RODD results for the MUSiC subcritical configurations," *American Nuclear Society Winter Meeting 2021*, **submitted** (2021).
12. F. DARBY and ET. AL., "Comparison of Neutron Multiplicity Counting Estimates with Trans-stilbene, EJ-309, and He-3 Detection Systems," *American Nuclear Society Winter Meeting 2021*, **submitted** (2021).
13. D. CIFARELLI and W. HAGE, "Models for a three-parameter analysis of neutron signal correlation measurements for fissile material assay," *Nuclear Instruments and Methods in Physics Research Section A: Accelerators, Spectrometers, Detectors and Associated Equipment*, **251**, *3*, 550 – 563 (1986).
14. R. FEYNMAN, F. D. HOFFMANN, and R. SERBER, "Dispersion of the neutron emission in U-235 fission," *Journal of Nuclear Energy (1954)*, **3**, *1*, 64 – IN10 (1956).
15. T. CUTLER, M. NELSON, and J. HUTCHINSON, "Deciphering the Binning Method Uncertainty in Neutron Multiplicity Measurements," *Transactions of the American Nuclear Society Winter Meeting* (2014).